Appl Phys A (2012) 108:177–183
DOI 10.1007/s00339-012-6868-8

Applied Physics A
Materials Science & Processing

Reversible resistance switching properties in Ti-doped polycrystalline Ta_2O_5 thin films

Xiliang He · Xiaomin Li · Xiangdong Gao · Weidong Yu · Rui Yang · Xinjun Liu · Xun Cao

Received: 26 August 2011 / Accepted: 19 January 2012 / Published online: 29 March 2012
© Springer-Verlag 2012

Abstract Unipolar reversible resistance switching effects were found in 5 at% Ti-doped polycrystalline Ta_2O_5 films with the device structure of Pt/Ti–Ta_2O_5/Pt. Results suggest that the recovery/rupture of the conductive filaments which are involved in the participation of oxygen vacancies and electrons leads to the resistance switching process. Ti-doped Ta_2O_5 thin films possess higher resistance whether in low-resistance state or high-resistance state and higher resistance switching ratio than Ta_2O_5 thin films, where Ti addition plays an important role in the resistance switching process by suppressing the migration of oxygen vacancies via forming an electrically inactive Ti/O–vacancy complex. Excellent retention properties of the high and low resistances under constant stress of applied voltage were obtained.

1 Introduction

Recently, resistance switching (RS) effects have been widely investigated and are expected to be used to fabricate the new generation of resistance random access memories (RRAMs) involved in nonvolatile data storage technologies [1, 2]. This RS phenomenon has been reported for a variety of materials such as transition-metal oxides [3, 4], perovskite oxides [5], solid electrolytes [6] and organic polymers [7]. Among them, simple binary transition metal oxides, such as NiO, TiO_2, Cu_2O and Ta_2O_5, are advantageous for their simple structure, constitution and compatibility with standard complementary metal oxide semiconductor processes. Various modes and mechanisms, such as conducting filaments [8, 9], the Schottky barrier model [10] and the Mott transition in insulators [11], have been proposed to describe and elucidate the RS behavior and its origin. Among them, the proposition of the formation and rupture of the filament conductive paths which consist of oxygen vacancies or metallic ions in the insulating matrix appears to be one of the most plausible. When it comes to Ta_2O_5 films, stoichiometric Ta_2O_5 films could be used as high-k dielectric materials [12] while nonstoichiometric Ta_2O_5 films could be used as solid electrolytes [13], which involve the participation of oxygen vacancies and conducting ions. Therefore, the RS properties of Ta_2O_5 films are expected, and some attention has been paid to them [14]. In this paper, the heterostructure Pt/Ti–Ta_2O_5/Pt was fabricated and its RS characteristics and resistance retention properties were investigated in detail. The mechanism of the RS effect referring to the formation/rupture of the conduction filaments and the effects of Ti addition are discussed.

X. He · X. Li (✉) · X. Gao · W. Yu · R. Yang · X. Liu · X. Cao
State Key Laboratory of High Performance Ceramics and Superfine Microstructures, Shanghai Institute of Ceramics, Chinese Academy of Sciences, 1295 Ding Xi Road, Shanghai 200050, People's Republic of China
e-mail: lixm@mail.sic.ac.cn
Fax: +86-021-52413122

X. He · R. Yang · X. Cao
Graduate School of the Chinese Academy of Sciences, 19A Yuquanlu, Beijing 100049, People's Republic of China

2 Experimental

A RRAM device of Pt/Ti–Ta_2O_5/Pt heterostructure was fabricated, as shown in Fig. 1a. Ta_2O_5 thin films with 5 at% Ti dopant were deposited onto Pt/Ti/SiO_2/Si substrates by pulsed laser deposition at 300 °C and 2 Pa oxygen pressure. The as-deposited Ti–Ta_2O_5 thin films were then rapidly thermally annealed at 650 °C for 5 min in oxygen ambient. The Pt top electrode of about 0.01 mm^2 in area was then deposited by e-beam evaporation with a shadow mask. Electrical measurements were carried out by an Agilent 2410 at

room temperature. The $I-V$ characteristic used in this work was recorded in the voltage-control mode. The annealed Ta_2O_5 and Ti-doped Ta_2O_5 thin films were determined to be of polycrystalline structure by X-ray diffraction (XRD, D/MAX-2550V). The sectional and surface morphologies of the Ta_2O_5 and Ti-doped Ta_2O_5 thin films before and after annealing were measured by field emission scanning electron microscopy (FESEM) and atomic force microscopy (AFM), respectively.

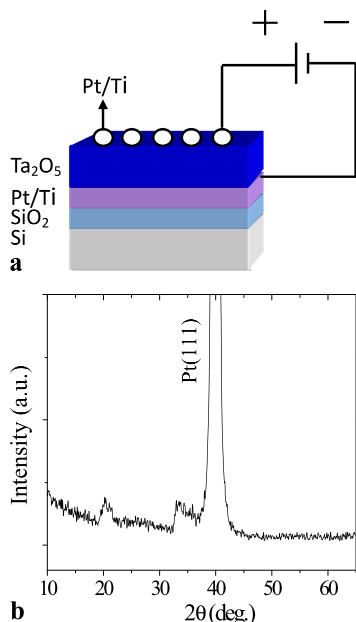

Fig. 1 (**a**) The sketch figure of the Pt/Ti–Ta_2O_5/Pt device heterostructure. (**b**) The XRD pattern of the annealed Ti-doped Ta_2O_5 thin film

3 Results and discussion

The structural properties of the annealed Ti–Ta_2O_5 thin film were measured by X-ray diffraction (XRD), and the result is shown in Fig. 1b, which is the same as that of the Ta_2O_5 thin film. As can be seen from the XRD spectra, the annealed Ti–Ta_2O_5 thin film has a very weak polycrystalline structure, though some peaks may have been hidden in the case of strong diffraction intensity of the Pt/Ti/SiO_2/Si substrate.

The sectional and surface scanning photographs were obtained by SEM and AFM for Ta_2O_5/Pt and Ti–Ta_2O_5/Pt devices before and after rapid thermal annealing (RTA) at 650 °C. The sectional and surface scanning photographs for the Ti–Ta_2O_5/Pt device are shown in Figs. 2a–2d, which are the same as those of the Ta_2O_5/Pt device. Before annealing, the film was dense and even textured, as shown in Fig. 2a. After annealing, the film had a polycrystalline-like structure, as shown in Fig. 2b. Before annealing, the surface of the film was smooth and compact, and the root mean square roughness was about 0.3 nm, as shown in Fig. 2c. After annealing, the surface of the film became coarse and there arose some tiny hollow-like structures, and the root mean square roughness increased to about 3.80 nm, as shown in Fig. 2d.

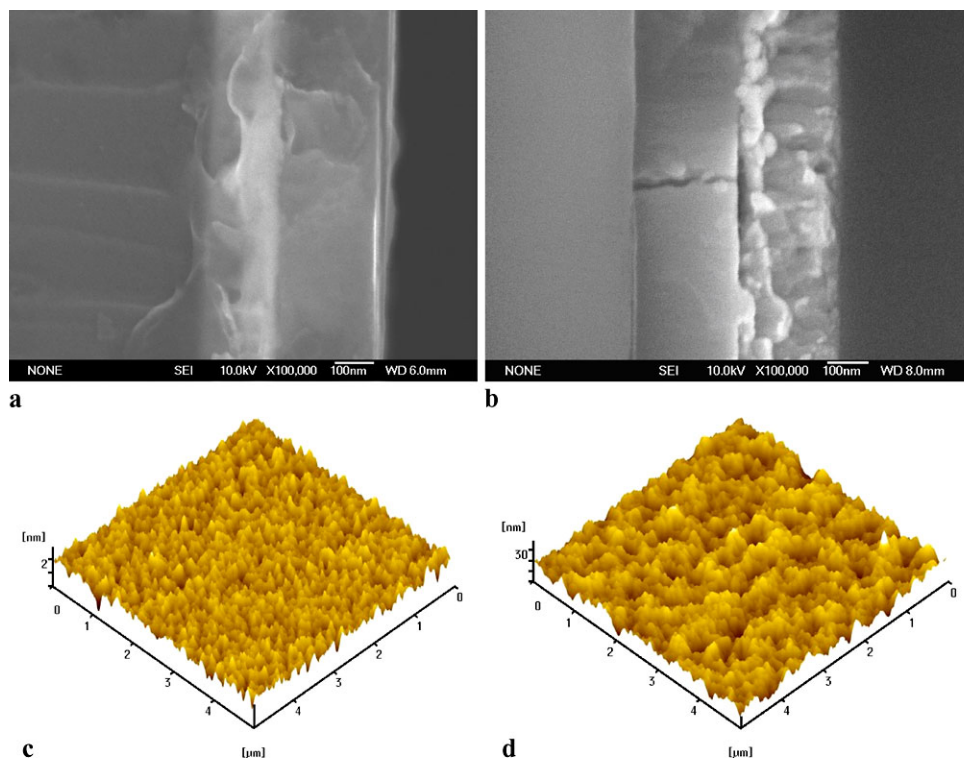

Fig. 2 SEM and AFM images of Ti-doped Ta_2O_5/Pt before and after rapid thermal annealing (RTA) at 650 °C. (**a**) SEM image before RTA, (**b**) SEM image after RTA, (**c**) AFM image before RTA, (**d**) AFM image after RTA

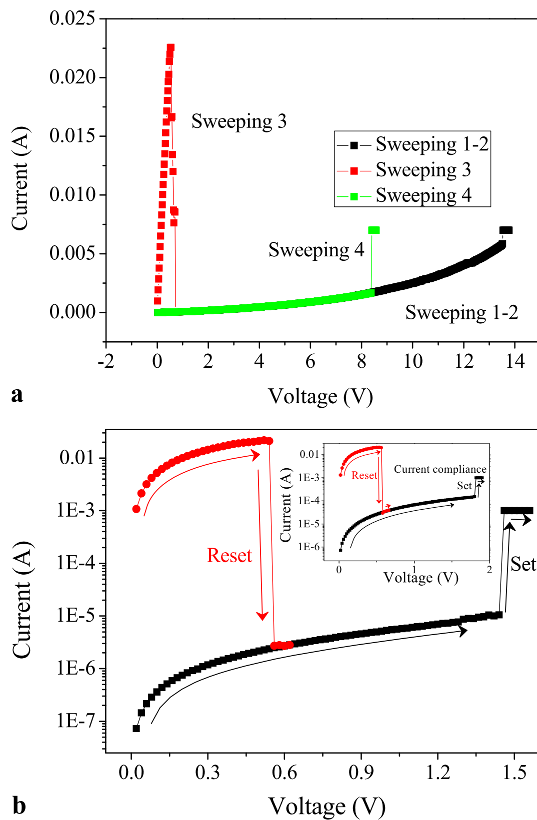

Fig. 3 (**a**) The first four I–V sweeping cycles for the Pt/Ti–Ta_2O_5/Pt device measured at room temperature; current flows from top Pt/Ti electrode to bottom Pt/Ti electrode in positive direction. (**b**) The stable I–V sampling curves of the Pt/Ti–Ta_2O_5/Pt heterostructure with the current compliance of 1 mA. The *inset graph* shows the I–V sampling curves of the Ta_2O_5 thin film without Ti doping with the same device structure as that of the Ti-doped Ta_2O_5 film

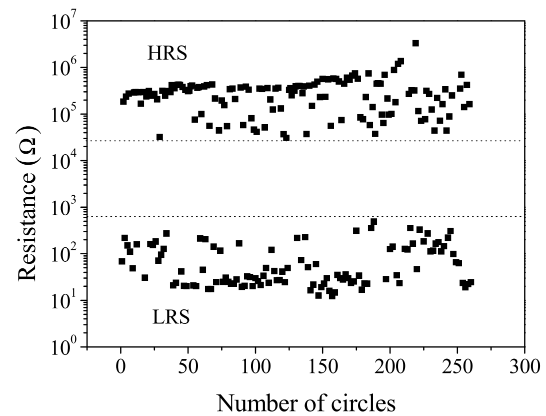

Fig. 4 The RS between HRS and LRS with the number of sweeping cycles

Figure 3a shows the first four current–voltage (I–V) sweeping cycles of the Pt/Ti/Ti–Ta_2O_5/Pt/Ti/SiO_2/Si device which were plotted in half-logarithmic form. As can be seen from the figure, the initial state of the sample was the high-resistance state (HRS). After two sweeping cycles, the sample entered the low-resistance state (LRS) until its current compliance. The current compliance was applied in order to prevent the permanent dielectric breakdown of the sample. The RS process was achieved without any forming operation, which refers to the so-called soft breakdown process.

Figure 3b shows the typical I–V characteristics in a half-logarithmic plot of the sample during a linear voltage sweep with the current compliance of 1 mA after the first four sweeping cycles. The inset shows the I–V characteristics of the undoped Ta_2O_5 film. The Ti-doped Ta_2O_5 thin film and the undoped Ta_2O_5 thin film have the same I–V characteristic. When applying the sweeping voltage from 0 V to positive values at a step of 0.02 V, the current suddenly increased by several orders of magnitude at about 1.4 V to the current compliance, the so-called set process, which switches the resistance of the sample from the HRS to the LRS. The positive voltage refers to the voltage applied on the top electrode with the bottom electrode grounded. Subsequently, applying the sweeping voltage from 0 V still to positive values at a step of 0.02 V, the current suddenly decreases by several orders of magnitude at about 0.6 V, the so-called reset process, which switches the resistance of the sample from the LRS to the HRS. The HRS and the LRS can be stable even after the removal of the applied voltage. The set and reset processes can also be realized by applying a negative voltage, which means that the RS behavior hardly depends on the polarity of the applied voltage, i.e. the 'unipolar switching' behavior.

Figure 4 shows the RS between the HRS and the LRS vs the number of sweeping cycles, in which a set or reset process is defined as a cycle. It is found that the RS ratio $[(R_{HRS} - R_{LRS})/R_{LRS}]$ is always larger than 5000 %, and most of them achieve 10^6 %. Such a huge resistance change ratio offers enough margin to distinguish between the two states, establishing two well-resolved states.

The RS characteristic suggests that the LRS of the Ta_2O_5 thin film was due to the filament conduction process [15]. The migration of the defects, i.e. oxygen vacancies, through the extended defects, such as the grain boundaries of the polycrystalline Ta_2O_5 thin film, forms the conducting filaments consisting of many tiny filaments, which are schematically shown in Fig. 5a. Figure 5b shows the schematic images of the many kinds of possible tiny filaments, which consist of oxygen vacancies as shown in Fig. 5c. Abundant oxygen vacancies exist in the film, which are deep double donors capable of producing two free electrons as follows:

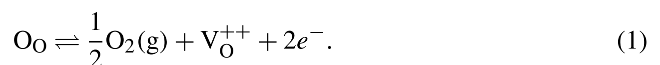

$$O_O \rightleftharpoons \frac{1}{2}O_2(g) + V_O^{++} + 2e^-. \quad (1)$$

When the external current density is high enough in the LRS, sufficient electrons are injected in the film to fill excess Ta^{5+} demand and suppress the existence of oxygen vacancies (compelling the process of Eq. (1) from right to left), forming a stoichiometric-like insulating Ta_2O_5 film

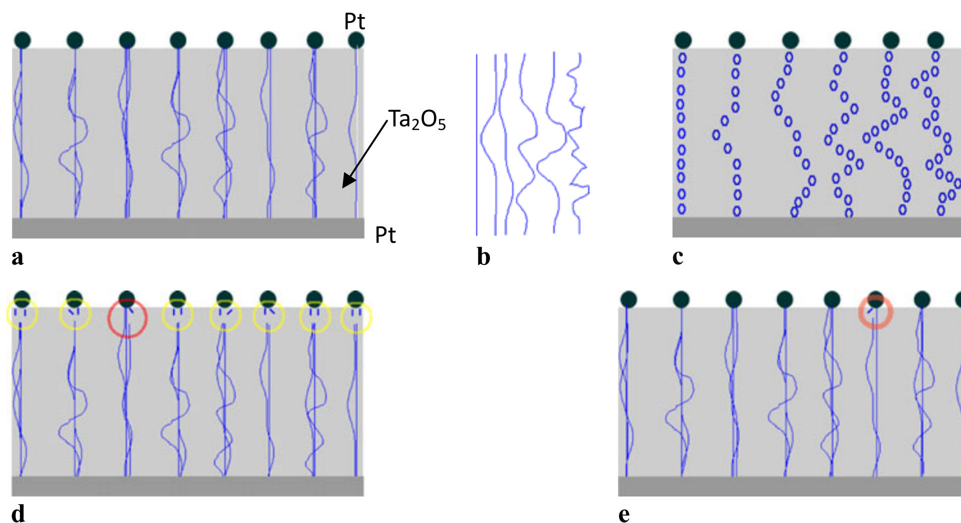

Fig. 5 (**a**) Schematic image of the generation of the conductive filaments which consist of many tiny filaments. (**b**) Schematic image of the many kinds of possible tiny filaments. (**c**) Schematic image of the filament consisting of oxygen vacancies. (**d**) Schematic image of the shift or rupture of conductive paths indicated by the *yellow circles* and the incomplete rupture part indicated by the *red circle*. (**e**) Schematic image of the recovery of the conductive filaments and the incomplete recovery part indicated by the *red circle*

and achieving the HRS, like a process of oxidation. During this process, Joule heating effects would highly elevate the conductance of the Ta_2O_5 thin film in the LRS according to the electrical transport mechanism, in which it would increase the external current density and accelerate the injection process of the electrons significantly. Subsequently, some parts of the tiny conductive paths shift or rupture leading to the rupture of all the conductive paths, which is schematically shown in Fig. 5d. The amounts of the ruptured tiny filaments and the degree of the suppression of the oxygen vacancies determine the states of the high resistance. As for the set process, under the inducement of the strong electrical field, the shifted or ruptured parts recover resulting in the generation/recovery of the conductive filaments, which is schematically shown in Fig. 5e. Plentiful electrons were transferred away from the film simultaneously which activated the oxygen vacancies that were suppressed by the electrons during the reset process, forming the nonstoichiometric-like Ta_2O_5 thin film and achieving the LRS, like a process of reduction, the reversible process of the oxidation.

Additionally, during the sweeping processes, some important characteristics of the set and reset processes were found, which could be helpful to understand the RS mechanism. Firstly, at the initial sweeping stage, the set voltage would become higher with the number of set cycles, until a set voltage of about 4 or 5 V, as shown in Fig. 6a, which is very similar to the so-called forming process. The next set voltage would be very low (∼1 or 2 V). The low set voltage suggests the incomplete reduction process, i.e. the incomplete rupture of all the tiny filaments, which is schematically shown in Fig. 5d indicated by the orange circle. The incomplete rupture may result from the changes of the oxygen vacancies' locations or the distance between them. After the forming-like process, which indicates a complete reduction, the next set voltage would reasonably be lower, which is in good agreement with the experimental results. Simultaneously, at the initial stages, the resistance of the LRS would reach more than 500 Ω, indicating the incomplete oxidation process, which is schematically shown in Fig. 5d indicated by the red circle. Secondly, if we define the process of the set voltage from the lowest to the highest as a period, the number of set voltages in each period would become less with the increasing of the periods, as shown in Figs. 6a and 6b. Thirdly, the lowest set voltage after each forming-like set voltage becomes lower with the increasing of the set periods. Fourthly, after about 10 set periods, the trends of the change of the set voltage and the forming-like set voltage vanish, and the set voltages are stable at about 1–2 V, as shown in Fig. 6c. After several forming-like processes, the oxidation–reduction zones relevant to the recovery/rupture of the conductive filaments are highly activated, forming the stable RS process. All of these characteristics demonstrate the conductive filaments in the RS process.

Comparing the RS process of the Ti-doped Ta_2O_5 films with that of the undoped films, it is found that the stability and durability of the Ti-doped Ta_2O_5 films were better. Additionally, the resistance of the Ti-doped Ta_2O_5 films was much higher whether in LRS or HRS, as shown in Fig. 7a and b and the RS ratio was higher than that of the undoped films, usually one or two orders of magnitude higher. Ti acts as an acceptor-type dopant, which can substitute for Ta and result in a single acceptor capable of producing a free hole,

$$\mathrm{Ti} \rightarrow \mathrm{Ti}_{\mathrm{Ta}}^{-} + \mathrm{h}^{+}. \tag{2}$$

At high temperatures, Ti and oxygen vacancies can move and they ionize and attract each other resulting in the formation of defect complexes. During the sweeping process, especially with the assistance of Joule heating effects, two Ti single acceptors complex with a doubly ionized oxygen

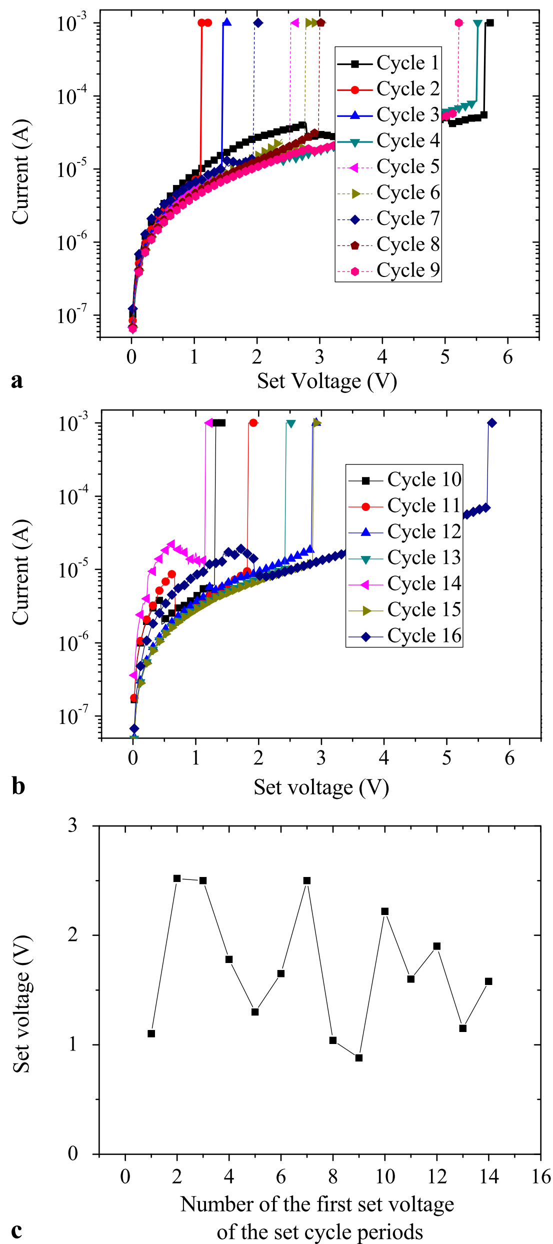

Fig. 6 (**a**) The changing trends of the set voltage in the first nine set processes. (**b**) The changing trends of the set voltage in the set cycle 10 to the set cycle 16. (**c**) Trends of the first set voltage in each set cycle period. We define the process of the set voltage from the lowest to the highest as a cycle period

vacancy to form an electrically inactive Ti/O–vacancy complex $Ti^{-}_{Ta} - V^{++}_{O} - Ti^{-}_{Ta}$ as follows [16]:

$$V_o + 2Ti \rightarrow Ti^{-}_{Ta} - V^{++}_{O} - Ti^{-}_{Ta}. \quad (3)$$

Therefore, Ti dopant can effectively suppress the migration of oxygen vacancies during the reset process and in HRS, in which it would highly elevate the oxidation degree and increase the insulating property of the Ta_2O_5 film. During the set process, the inactive Ti/O–vacancy complex would be taken apart by the drift of the free electrons.

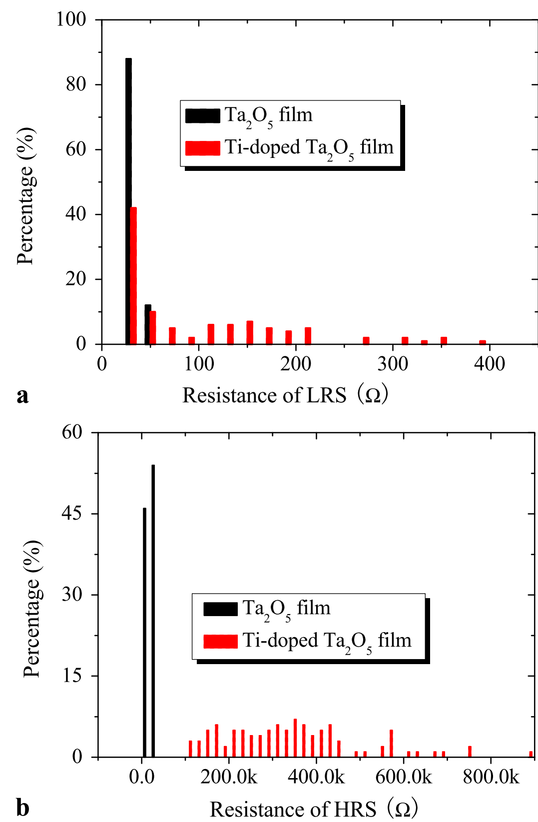

Fig. 7 (**a**) The percentage distribution comparison of the LRS between Ti-doped Ta_2O_5 thin film and undoped Ta_2O_5 thin film. (**b**) The percentage distribution comparison of the HRS between Ti-doped Ta_2O_5 thin film and undoped Ta_2O_5 thin film. The columns in (**a**) and (**b**) represent the percentage of the resistance state within the same interval, i.e. 20 Ω for LRS and 20 KΩ for HRS

The retention properties of the resistance of the two well-resolved states of Ti-doped Ta_2O_5 thin films under the durable constant stress of 100 mV were measured and are plotted as shown in Figs. 8a–8c. Figure 8a shows the retention of HRS of Ti-doped Ta_2O_5 thin films at the initial stage of I–V sweeping. As can be seen from Fig. 8a, the resistance value of HRS remains the same for about 2100 s and then it switches into LRS. Figure 8b is the retention of HRS of Ti-doped Ta_2O_5 thin films after 20 I–V sweeping processes. As can be seen from Fig. 8a, the resistance value of HRS remains the same for about 3600 s and then it switches into LRS. The resistance value of LRS remains the same for about 2000 s and then it switches into HRS again. Figure 8c shows the retention of HRS and LRS of Ti-doped Ta_2O_5 thin films after 250 I–V sweeping processes. As can be seen from Fig. 8c, the resistance values of HRS have a slowly increasing process at the first stage of about 15000 s and then become quite steady after that. The increasing process reasonably corresponds to the progressive reduction process until the complete reduction, consistent with the analysis of the conducting mechanism above. Relatively, the values of the LRS almost stayed the same dur-

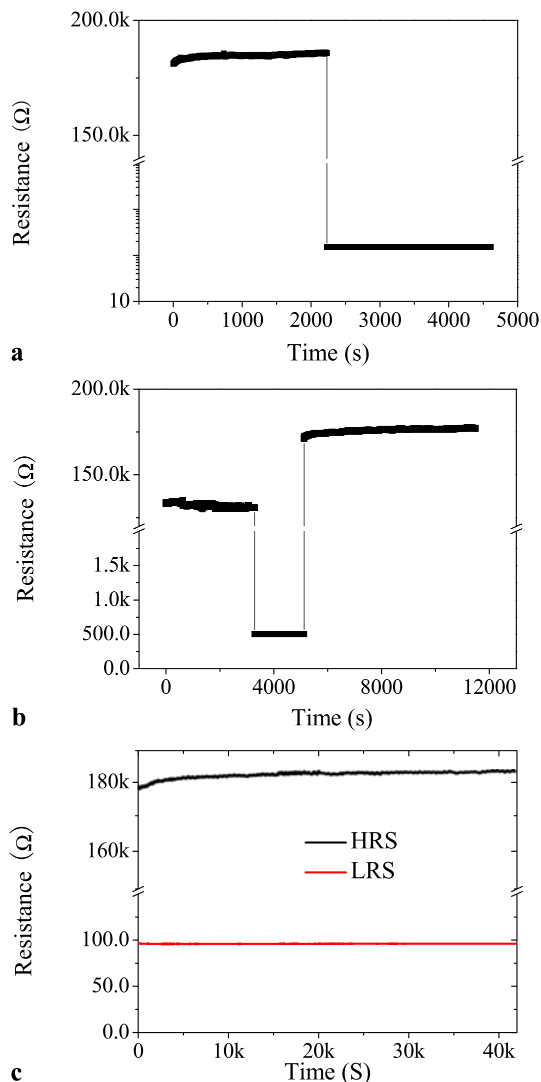

Fig. 8 Retention properties of HRS and LRS of Pt/Ti–Ta_2O_5/Pt heterostructure under the durable constant stress of 100 mV as a function of the stress time at different sweeping stages. (**a**) Retention of HRS, at initial sweeping stage; (**b**) retention of HRS, after 20 I–V sweeping cycles; (**c**) retention of HRS and LRS, after 250 I–V sweeping cycles, at the stable RS stage

ing the stressing time. And, during the evolution process, the ratio of the HRS to the LRS is higher than 150000 % and increases with the stress time. At the initial sweeping process stage, the RS properties are unstable and the oxidation/reduction processes are incomplete, which means that the recovery/rupture (shift) of the conductive filaments is incomplete, leading to the switches of the resistance state during the retention measurements. After a period of sweeping processes, the oxidation/reduction processes become complete, which means that the recovery/rupture (shift) of the conductive filaments is complete, resulting in the excellent retention properties of HRS and LRS. Therefore, the retention properties greatly support the switching mechanism of Ta_2O_5 thin films in this work.

4 Conclusions

In summary, the heterostructure of Pt/Ti–Ta_2O_5/Pt with a polycrystalline Ta_2O_5 film was fabricated and its resistance switching properties for the application in nonvolatile memories were investigated. Unipolar RS properties of Pt/Ti–Ta_2O_5/Pt with resistance switching ratio larger than 5000 % and excellent retention behavior for more than 12 h under the continuous voltage were obtained. Compared to Ta_2O_5 films, Ti-doped Ta_2O_5 films exhibited higher LRS or HRS values and higher resistance switching ratio, where Ti addition plays an important role in the RS process by suppressing the migration of oxygen vacancies via forming the inactive Ti/O–vacancy complex. The RS characteristics indicate that the switching resulted from the recovery/rupture of the conductive filaments which consisted of many tiny filaments. Not all of the tiny filaments recover/rupture in the same set/reset process, which refers to the incomplete oxidation/reduction process, especially at the initial stage of the RS process. This work highlights the potential advantages of the doping technique of oxide films in realizing highly stable RRAM devices with excellent RS properties.

Acknowledgements This work is financially supported by the Shanghai–AM Research and Development Fund (No. 08700740900), the Natural Science Foundation of Shanghai (No. 08ZR1421500) and the Keystone Project of Shanghai Basic Research Program (No. 08JC1420600).

References

1. J.J. Yang, M.D. Pickett, X. Li, D.A.A. Ohlberg, D.R. Stewart, R.S. Williams, Nat. Nanotechnol. **3**, 429 (2008)
2. W.W. Zhuang, W. Pan, B.D. Ulrich, J.J. Lee, L. Stecker, A. Burmaster, D.R. Evans, S.T. Hsu, M. Tajiri, A. Shimaoka, K. Inoue, T. Naka, N. Awaya, K. Sakiyama, Y. Wang, S.Q. Liu, N.J. Wu, A. Ignatiev, in *Tech. Dig. Int. Electron Devices Meet.* (2002), p. 193
3. S.-E. Ahn, M.-J. Lee, Y. Park, B.S. Kang, C.B. Lee, K.H. Kim, S. Seo, D.-S. Suh, D.-C. Kim, J. Hur, W. Xianyu, G. Stefanovich, H. Yin, I.-K. Yoo, J.-H. Lee, J.-B. Park, I.-G. Baek, B.H. Park, Adv. Mater. **20**, 924 (2008)
4. K. Tsunoda, Y. Fukuzumi, J.R. Jameson, Z. Wang, P.B. Griffin, Y. Nishi, Appl. Phys. Lett. **90**, 113501 (2007)
5. Y.B. Nian, J. Strozier, N.J. Wu, X. Chen, A. Ignatiev, Phys. Rev. Lett. **98**, 146403 (2007)
6. T. Sakamoto, H. Sunamura, H. Kawaura, T. Hasegawa, T. Nakayama, M. Aono, Appl. Phys. Lett. **82**, 3032 (2003)
7. A. Ranman, M.K. Sanyal, Nanotechnology **19**, 395203 (2008)
8. C. Yoshida, K. Tsunoda, H. Noshiro, Y. Sugiyama, Appl. Phys. Lett. **91**, 223510 (2007)
9. B.J. Choi, S. Choi, K.M. Kim, Y.C. Shin, C.S. Hwang, Appl. Phys. Lett. **89**, 012906 (2006)
10. T. Fujii, M. Kawasaki, A. Sawa, Y. Kawazoe, H. Akoh, Y. Tokura, Phys. Rev. B **75**, 165101 (2007)
11. D.S. Kim, Y.H. Kim, C.E. Lee, Y.T. Kim, Phys. Rev. B **74**, 174430 (2006)

12. W.S. Lau, K.K. Khaw, T. Han, N.P. Sandler, Appl. Phys. Lett. **89**, 262901 (2006)
13. M.T. Seman, J.J. Robbins, D. Leonhardt, S. Agarwal, C.A. Wolden, J. Electrochem. Soc. **155**, 168 (2008)
14. J.J. Yang, M.-X. Zhang, J.P. Strachan, F. Miao, M.D. Pickett, R.D. Kelley, G. Medeiros-Ribeiro, R.S. Williams, Appl. Phys. Lett. **97**, 232102 (2010)
15. F. Miao, J.P. Strachan, J.J. Yang, M.-X. Zhang, I. Goldfarb, A.C. Torrezan, P. Eschbach, R.D. Kelley, G. Medeiros-Ribeiro, R.S. Williams, Adv. Mater. **23**, 5633 (2011)
16. M.-J. Lee, C.B. Lee, D. Lee, S.R. Lee, M. Chang, J.H. Hur, Y.-B. Kim, C.-J. Kim, D.H. Seo, S. Seo, U.-I. Chung, I.-K. Yoo, K. Kim, Nat. Mater. **10**, 625 (2011)